Depolarization Increases the Single-Channel Conductance and the Open Probability of Crayfish Glutamate Channels

O. Tour, H. Parnas, and I. Parnas

Otto Loewi Center for Cellular and Molecular Neurobiology, and Department of Neurobiology, The Hebrew University, Jerusalem, Israel 91904

ABSTRACT We have studied the voltage sensitivity of glutamate receptors in outside-out patches taken from crayfish muscles. We found that single-channel conductance, measured directly at the single-channel level, increases as depolarization rises. At holding potentials from −90 mV to ~20 mV, the conductance is 109 pS. At holding potentials positive to 20 mV, the conductance is 213 pS. This increase in single-channel conductance was also observed in cell-attached patches. In addition, desensitization, rise time, and the dose-response curve were all affected by depolarization. To further clarify these multifaceted effects, we evaluated the kinetic properties of single-channel activity recorded from cell-attached patches in hyperpolarization (membrane potential around −75 mV) and depolarization (membrane potential ~105 mV). We found that the glutamate dissociation rate constant (k_-) was affected most significantly by membrane potential; it declined 6.5-fold under depolarization. The rate constant of channel closing (k_c) was also significantly affected; it declined 1.8-fold. The rate constant of channel opening (k_o) declined only 1.2-fold. The possible physiological significance of the depolarization-mediated changes in the above rate constants is discussed.

INTRODUCTION

Studies of ligand-gated ion channels revealed that some channels exhibit voltage sensitivity. A pioneering work in this direction concerns the nicotinic acetylcholine receptor (Magleby and Stevens, 1972). The dependence of the conductance of the *N*-methyl-D-aspartate (NMDA) receptor on membrane potential, via a Mg^{2+} open channel block, is well established (Nowak et al., 1984; Mayer and Westbrook, 1984). It is this dependence that underlies the role attributed to the NMDA receptor in learning and memory (Watkins, 1994).

Concerning non-NMDA glutamate receptors, it was found, in some vertebrate preparations, that the α-amino-3-hydroxy-5-methyl-4-isoxazolepropionate (AMPA) receptor is also voltage sensitive. The voltage sensitivity has been attributed to block by polyamines (Bowie and Mayer, 1995), to voltage dependence of gating (Jonas and Sakmann, 1992; Raman and Trussell, 1995), and to voltage dependence of desensitization (Patneau et al., 1993). In other preparations, however, the *I-V* relation was found to be nearly linear (Hestrin et al., 1990; Keller et al., 1991; Colquhoun et al., 1992; Livsey et al., 1993).

In invertebrates, the quisqualate type of glutamate receptor in crayfish was found to be voltage dependent (Dudel, 1974; Onodera and Takeuchi, 1978; Dudel, 1979; Dudel and Franke, 1987), but the exact mechanism underlying this voltage dependence has not yet been fully elucidated.

Here we examine, in detail, the voltage dependence of the glutamate receptor of crayfish muscle. Our direct measurements at the single-channel level show that membrane potential affects channel conductance. Furthermore, we show that membrane potential also affects the probability of channel opening (P_o).

Received for publication 19 May 1997 and in final form 13 January 1998.

Address reprint requests to Dr. O. Tour, Department of Neurobiology, The Hebrew University, Jerusalem, Israel 91904. Tel.: 972-2-658-5900; Fax: 972-2-652-1921; E-mail: tour@vms.huji.ac.il.

0006-3495/98/04/1767/12 $2.00

MATERIALS AND METHODS

Preparation and solutions

Deep abdominal extensor muscles (Parnas and Atwood, 1966) were isolated from crayfish (*Procambarus clarki*) 4–8 cm in length. They were bathed in the standard Van Harreveld solution containing 220 mM NaCl, 5.4 mM KCl, 13.5 mM $CaCl_2$, 2.5 mM $MgCl_2$, and 10 mM Tris-maleate buffer, with the pH adjusted to 7.4 with NaOH. Patch electrodes for outside-out recordings were filled with low Cl^- intracellular solution that contained 150 mM K-propionate, 5 mM Na-propionate, 10 mM $MgCl_2$, 10 mM EGTA to establish a low Ca^{2+} concentration of 10^{-8} M, and 10 mM Tris-maleate buffer, with the pH adjusted to 7.2 by adding KOH. For cell-attached recordings, the electrodes were filled with the standard Van Harreveld solution, which contained glutamate (L-glutamic acid sodium salt; BDH, Poole, England).

Fast application technique

The fast application system used for applying pulses of glutamate to outside-out patches has been described in detail previously (Franke et al., 1987; Dudel et al., 1990). Briefly, solution containing agonist was ejected by pressure from a polyethylene tube, which was glued to a steel needle to form a well-defined thin liquid filament. The tube was moved rapidly by a piezocrystal so that the liquid filament washed the tip of a patch pipette within 200 μs (Tour et al., 1995). Even though the rate of removal of glutamate is not relevant to any of the experiments presented here, it should be noticed that the removal of glutamate was less rapid.

Patch-clamp recording

The muscles were treated with 0.3 mg/ml collagenase (Sigma; type Ia) for 20 min at 20–22°C. The patch-clamp technique (Hamill et al., 1981) was used both in the outside-out and cell-attached configurations. Thin-wall

borosilicate capillaries with an inner filament (GC150TF-10; CEI, Pangbourne, England), were pulled in two stages with a computerized DMZ horizontal pipette puller (Augsburg, Germany). Pipette resistance was 2–7 MΩ. For cell-attached experiments, electrodes were coated with Sylgard (type 182; Dow Corning, Seneffe, Belgium).

For the outside-out patches, the activity of 1–20 glutamate channels was recorded (Axopatch-1c; Axon Instruments, Foster City, CA), filtered at 2 kHz, and stored on a video cassette connected via a neuro-corder (Neurodata, New York, NY) with a 100-kHz sampling rate A/D conversion. Data were fed off-line (TL-1 or DigiData 1200 interfaces; Axon Instruments) at 20 kHz and analyzed with pCLAMP6 software (Axon Instruments).

For the cell-attached patches, filtration was at 10 kHz, and off-line feeding of the data was at 100 kHz. For data analysis only, patches with less than 0.4 pA RMS noise were used.

Electrical artifacts and leak currents were eliminated from the glutamate-activated ensemble currents by subtracting jump responses and voltage protocols recorded in the absence of glutamate.

To overcome possible distortion of the results by rundown, the various experimental treatments were conducted in an alternate fashion.

The averaged data are given as mean ± SD.

RESULTS

Basic findings

Fig. 1 depicts the basic findings. Two aspects are apparent. First the current amplitude increases, and second the decay of the current is slowed as the membrane holding potential (HP) becomes more positive (Fig. 1 *A*).

From experiments like the one shown in Fig. 1 *A*, the dependence of the peak current (I_p) on a wide range of HPs (−90 mV to 90 mV) was established. Fig. 1 *B* depicts normalized average results from four experiments. The curve slope remains constant at the range of −90 mV to 30 mV, and the reversal potential is 10 mV. At HPs higher than 30 mV, a continuous rise in the curve slope is seen.

To clarify the mechanism underlying the dependence of I_p on HP, we recall the relationship in Eq. 1, derived from Ohm's law.

$$I_p = \gamma(\mathrm{HP} - V_r) \times N \times P_{O_{(peak)}} \quad (1)$$

where γ is the single-channel conductance, V_r is the reversal potential, N is the number of channels in the patch, and $Po_{(peak)}$ is the open probability at the time of the peak current.

Equation 1 shows that the results seen in Fig. 1 *B* can be attributed to a dependence of γ and/or $Po_{(peak)}$ on HP.

Dependence of γ on HP

To check for γ, an *I-V* curve ranging from −90 mV to 90 mV was obtained from experiments of the type shown in Fig. 2 *A*. In particular, single-channel currents from outside-out patches were measured at various HPs. Fig. 2 *A* shows that, for pairs with the same driving force, the current amplitudes are significantly higher at the higher depolarizations (cf. *left and right traces*). A full *I-V* curve (average of four experiments) is given in Fig. 2 *B*. Two slopes (i.e., conductances) with an inflection at ~20 mV are seen. Linear regression lines for the ranges of −90 mV to −30 mV and 20 mV to 90 mV yield slopes of 109 pS and 213 pS ($R > 0.99$), respectively. Thus γ is about double at depolarizations higher than 20 mV.

To ensure that the increase in γ reflects an intrinsic property of the channels, *I-V* curves were also measured using the cell-attached configuration. Fig. 2 *C* shows an average *I-V* curve using cell-attached patches ($n = 5$). A similar increase in γ is seen; for command potentials at the range of 80 mV to −60 mV (patch potential of ~ −155 mV to −15 mV), the conductance is 100 pS, whereas for com-

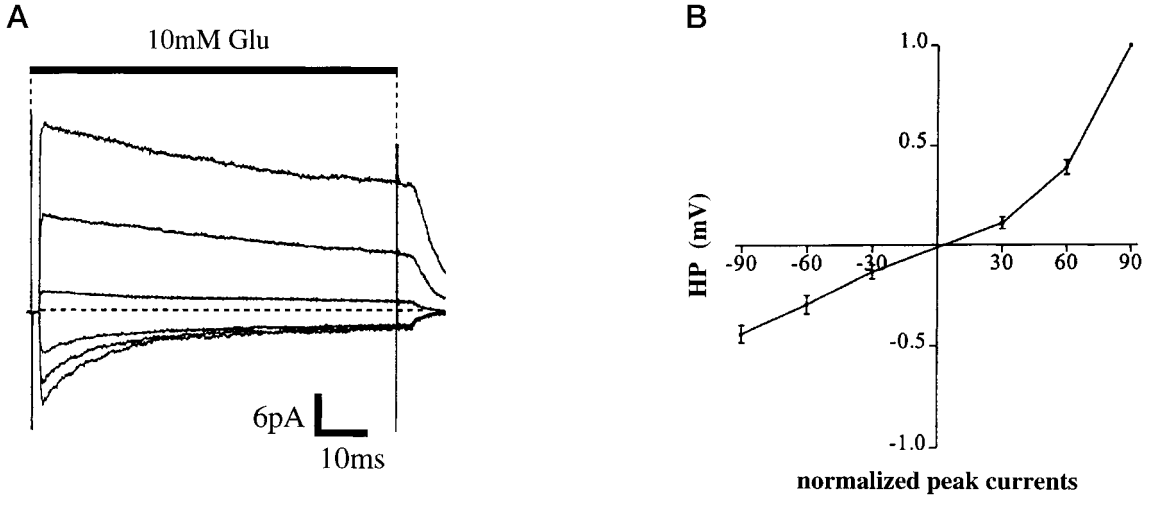

FIGURE 1 Outside-out patch recordings. (*A*) Ensemble currents activated by a 100-ms pulse of 10 mM glutamate at six different membrane holding potentials (−90 mV, −60 mV, −30 mV, 30 mV, 60 mV, and 90 mV). Each trace is the outcome of averaging 130 responses. The dashed line indicates zero current. Here and in the following figures, the horizontal thick bar and vertical dotted lines indicate the duration of glutamate application. (*B*) Normalized (to the 90-mV current) peak currents to voltage relation obtained with the same experimental protocol as in *A*. Average of four experiments.

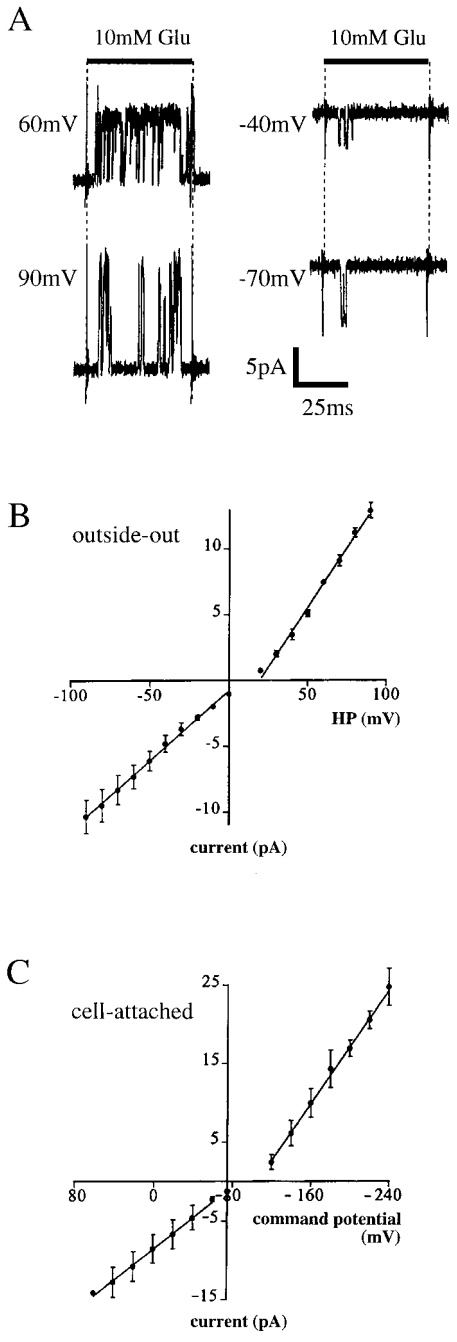

FIGURE 2 Increase of single-channel conductance with depolarization. (*A*) Examples of single-channel currents from the same outside-out patch at four HPs. The driving force (reversal potential ≅ 10 mV) is identical in the upper pair (60 mV, −40 mV) and lower pair (90 mV, −70 mV). (*B*) An averaged *I-V* curve ($n = 4$) ranging from −90 mV to 90 mV extracted from data of the type seen in *A*. The numbers of averaged measurements for the potentials (in mV) −90, −80, −70, −60, −50, −40, −30, −20, −10, 0, 20, 30, 40, 50, 60, 70, 80, 90, are 3, 3, 3, 3, 4, 3, 4, 2, 1, 1, 1, 3, 4, 4, 4, 3, 3, 4, 3, respectively. Linear regression lines for the ranges of −90 mV to −30 mV and 20 mV to 90 mV yield slopes of 109 pS and 213 pS ($R > 0.99$), respectively. (*C*) An averaged ($n = 5$) *I-V* curve constructed from single-channel recordings from cell attached patches. Command potential varied between 60 mV (hyperpolarization) to −240 mV (depolarization). Assuming a resting potential of ~75 mV, the membrane potential range is −135 mV to 165 mV). The numbers of averaged measurements for the command potentials (in mV) −240, −220, −200, −180, −160, −140, −120, −60, −40, −20, 0, 20, 40, 60 are 2, 4, 4, 5, 5, 5, 2, 2, 4, 4, 5, 4, 4, 2, respectively. Linear regression lines for the ranges of 60 mV to −60 mV and −120 mV to −240 mV yield slopes of 100 pS and 184 pS ($R > 0.99$), respectively. The polarities of the registered currents were reversed to conform to the outside-out measurements.

mand potentials at the range of −120 mV to −240 mV (patch potential of ~45 mV to 165 mV), γ is 184 pS. The reversal potential is ~15 mV.

The following experiments show that the increase in γ with an increase in depolarization cannot alone account for the results seen in Fig. 1 *A*.

Dependence of the open probability (P_o) on HP

Fig. 3 *A* depicts examples of traces where 10 mM glutamate was applied at two HPs of −80 mV (*left column*) and 80 mV (*right column*). In this outside-out patch the activity of only one channel was seen. It is apparent that P_o is higher at the 80 mV. As seen, at 80 mV the channel spends a larger fraction of the glutamate application time at the open state (see also Fig. 2 *A*). This reflects the fact that P_o is higher, at 80 mV, throughout the application period and not only at the peak current. Moreover, channels were opened in 86 of 100 repetitions at 80 mV. This should be compared to 46 of 100 repetitions at −80 mV (see *upper trace* as an example for a trace without openings). Because almost all openings occur in the beginning of the application period, this should lead to an increase in $Po_{(peak)}$ of ~60% at 80 mV.

One way of quantifying the results seen in Fig. 3 *A* is to construct an "all-points amplitude histogram" for the two HPs (Fig. 3 *B*). Each histogram was constructed from the amplitude values of all of the sampled points in 100 episodes at each HP (*80 mV right histogram and −80 mV left histogram*).

P_o can be extracted from Fig. 3 *B* by

$$N \times P_o = \frac{\sum_1^n \Delta t \times A_n \times (n-1)}{T} \qquad (2)$$

Here N is the number of channels in the patch, n is the number of peaks in the histogram, Δt is the sampling interval, A_n is the area below peak n and T is the total time of glutamate application.

The number of channels, N, in a patch is not known. However, for measurements at various HPs from the same patch, the number of channels is equal. Under these conditions a relative P_o can be extracted by using Eq. 2. In Fig. 3 *B*, P_o at HP of 80 mV is more than threefold larger than that at −80 mV, reflecting the entire increase in P_o with depolarization.

Fig. 3 *C* depicts an all-points amplitude histogram for a lower concentration of glutamate (1 mM). Each histogram was constructed from the amplitude values of all of the sampled points in 12 episodes at each HP. Multiple peaks (marked with an *asterisk*) in the right histogram represent the simultaneous openings of up to three channels, as compared to the rare simultaneous openings of two channels in

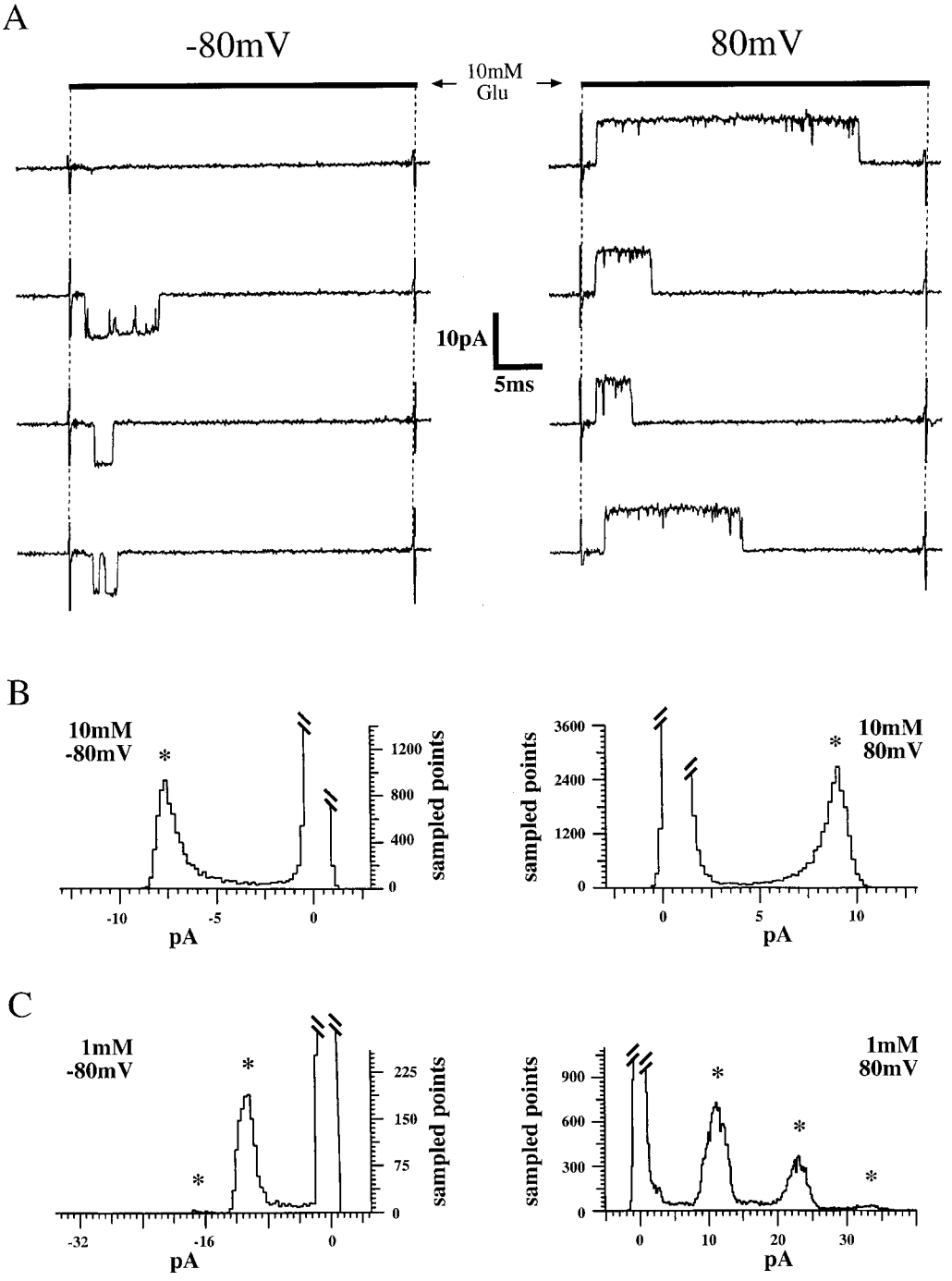

FIGURE 3 Increase in P_o with depolarization exemplified by single-channel measurements. (*A*) Left column: Four traces of single-channel currents at HP of −80 mV. No channel opening was recorded in the first trace. Right column: Four traces of single-channel currents at 80 mV. All recordings are from the same patch. (*B*) Two "all-point amplitude histograms" at HPs of 80 mV and −80 mV (*right* and *left*, respectively). Each histogram was constructed from the amplitude values of all sampled points (187,500 for each histogram) taken from 100 traces of 37.5-ms applications of 10 mM glutamate. The asterisks denote the location of the peaks. (*C*) As in *B*, but for all sampled points (12,000 for each histogram) taken from 12 60-ms applications of 1 mM glutamate. Notice that in all histograms the highest peak (*clipped*) is seen around zero pA.

the left histogram. Using Eq. 2, P_o at HP of 80 mV was found to be 7.8-fold larger than that at −80 mV. Comparing this value to the one obtained at 10 mM glutamate (threefold increase) clearly demonstrates that the increase in P_o at positive HPs is larger at lower glutamate concentrations.

Dependence of the decay phase on HP

Attempts to fit the decay phase of the currents seen in Fig. 1 *A* by a single exponent show that the time constant of decay increases as HP becomes more positive. However,

whereas a single exponent was reasonably adequate to describe the currents at extreme HPs, it failed to do so at intermediate ones.

In the extreme HPs, where a single exponent reasonably described the decay phase, we noticed two groups of time constants: one in the range of the more negative HPs (τ_H) and another for the more positive ones (τ_D). That is, average values of τ_H of 11.1 ± 3.1 ms and 11.7 ± 3.8 ms were obtained for HPs of −90 mV and −60 mV, respectively ($n = 9$). For the positive HPs of 90 mV and 60 mV, measured from the same nine patches, the average values of τ_D were 34.8 ± 16.4 ms and 33.2 ± 12.3 ms, respectively. Differences in the measured time constant among patches are a common observation when outside-out patches are used (Franke et al., 1993). The large variance partly reflects these differences. However, for a single patch τ_H was always shorter than τ_D. The average ratio (for nine patches) $(\tau_D)/(\tau_H)$ was 3.14 ± 1.09.

Based on the above and recalling that at least two exponents are needed to describe desensitization at intermediate HPs, we suggest below to fit the currents at all HPs with two exponents according to

$$I(t) = A_1 \times \exp^{-t/\tau_1} + A_2 \times \exp^{-t/\tau_2} + C \qquad (3)$$

We further suggest that τ_1 and τ_2 remain fixed for all HPs (where $\tau_1 = \tau_H$ and $\tau_2 = \tau_D$) while the amplitudes, A_1 and A_2, and the constant, C, vary with HP.

Fig. 4 shows currents, from a single patch, at HPs of −90 mV (*A*), −30 mV (*B*), and 90 mV (*C*). Using the approach described above, the value of τ_H (11.7 ms) was obtained from a best fit of a single exponent to the current at −90 mV (Fig. 4 *A*), and the value of τ_D (32 ms) was obtained from a best fit of a single exponent to the current at 90 mV (Fig. 4 *C*). Establishing τ_1 and τ_2 from the above and keeping them fixed, we fit two exponents to each of the currents (including currents at extreme HPs), and A_1 and A_2 were derived using Eq. 3. The solid lines in Fig. 4, *A–C*, which are indistinguishable from the data, even in the intermediate HP (Fig. 4 *B*) demonstrate the adequacy of our suggested procedure. This procedure was repeated for six patches, and the average results, expressed as $A_1/(A_1 + A_2)$, are seen in Fig. 4 *D*. It is quite apparent that at negative HPs, A_1 dominates, whereas A_2 dominates at positive HPs.

A qualitative dependence of *C* (Eq. 3) on HP is depicted in Fig. 5 *A*. Here the currents seen in Fig. 1 *A* were normalized, each to its own peak current. Furthermore, for convenience, the negative currents are shown as positive ones. In Fig. 5 *A*, the constant *C* of Eq. 3 is roughly reflected by the level of the current at the end of the glutamate application. It can be seen that *C* rises as HP becomes more positive (the lowest steady-state current is at an HP of −90 mV). A quantitative dependence of *C* on HP for these currents can be seen in Fig. 5 *B*. *C* was extracted from Eq. 3 (for $t \rightarrow \infty$), where τ_1 and τ_2 were determined as described above.

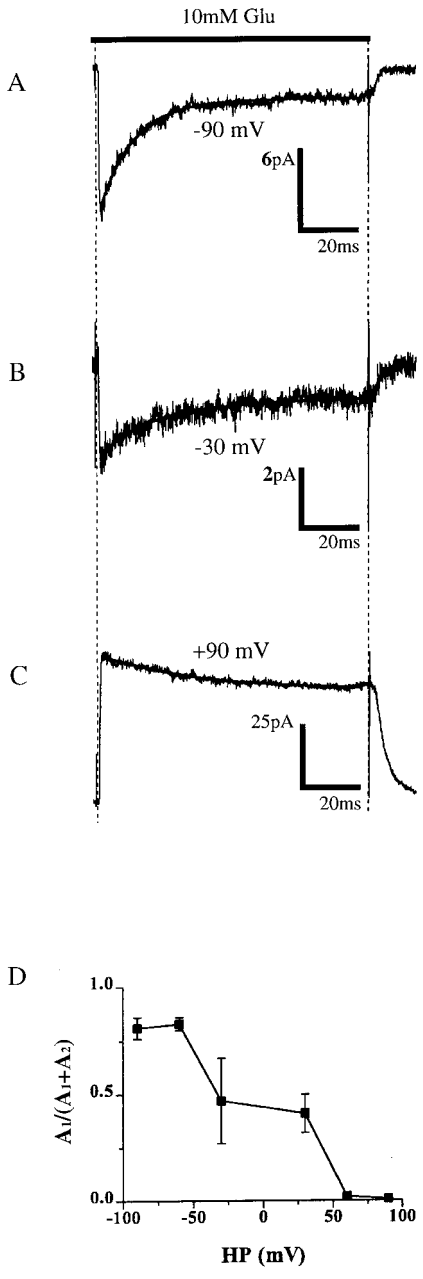

FIGURE 4 Dependence of the decay of the current on HP. *A*, *B*, and *C* are ensemble currents recorded from one patch at HPs of −90 mV, −30 mV, and 90 mV, respectively. Each trace is the outcome of averaging 60 repetitions. The decay phase was fitted (*solid line*) by a double exponent (Eq. 3) with τ_1 and τ_2 fixed ($\tau_1 = 11.7$ ms, $\tau_2 = 32$ ms; see text for details) and the amplitudes and the function constant, *C*, were varied. (*D*) Results (averaged) from six patches. $A_1/(A_1 + A_2)$ was calculated for various HPs. A_1 dominates at negative HPs, whereas A_2 dominates at positive HPs.

The exact meaning of the steady-state current (*C*) from the point of view of the involved rate constants is highly model dependent. A speculation concerning the possible meaning of *C* cannot be produced at this stage of the research.

The finding shown in Figs. 4 and 5 that A_2 and *C* increase as HP becomes more positive was confirmed in all six patches that were analyzed in this way.

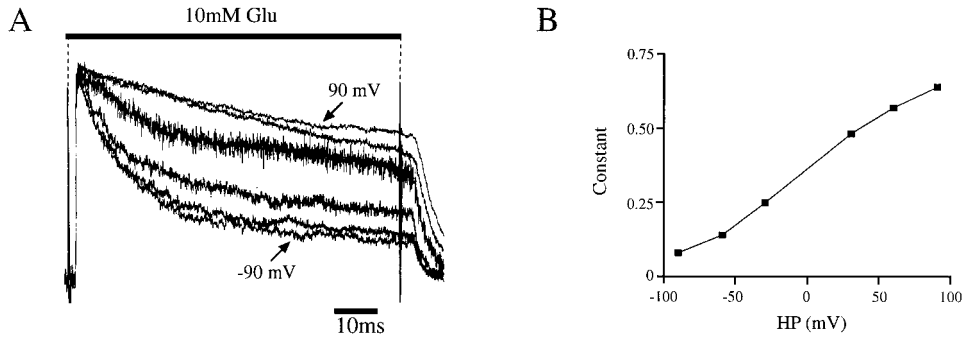

FIGURE 5 The dependence of C (the constant in Eq. 3) on HP. (*A*) The currents in Fig. 1 *A* were each normalized to their own peaks. For convenience, the negative currents appear as positive ones. C (Eq. 3), roughly reflected by the level of the current at the end of the glutamate application, rises as HP becomes more positive. (*B*) A quantitative representation of C as a function of HP for the currents in *A*.

Quantitative dependence of P_o on HP

As shown before, the current is not constant during the time of agonist application, but varies with time (Figs. 1 *A* and 4 *A–C*). Hence, to find the dependence of P_o on HP, we need to evaluate $P_o(t)$ at the various HPs. To do so, we must first extend Eq. 1 to include the time course of the current. To demonstrate the dependence of $I(t)$ and hence $P_o(t)$ on HP in a succinct quantitative way, we integrate the extended Eq. 1 to obtain

$$\int_0^t I(t)\mathrm{d}t = \gamma(\mathrm{HP} - V_r) \times N \times \int_0^t P_o(t)\mathrm{d}t \qquad (4)$$

To isolate $\int_0^t P_o(t)\mathrm{d}t$, we must first cancel the other dependencies on HP, as done in Fig. 6 *A*. Specifically, for each HP Eq. 4 is divided by $\gamma(\mathrm{HP} - V_r)$, corresponding to the relevant HP (Eq. 5), which is, in fact, the single-channel current at the specific HP (seen in Fig. 2 *B*):

$$\frac{1}{\gamma_{(\mathrm{HP})}(\mathrm{HP} - V_r)} \times \int_0^t I_{(\mathrm{HP})}(t)\mathrm{d}t = N \times \int_0^t P_{o(\mathrm{HP})}(t)\mathrm{d}t \qquad (5)$$

Examples that demonstrate this procedure are seen in Fig. 6 *A*. Two extreme HPs from Fig. 1 *A* were each divided by the single-channel current recorded at it's HP (taken from Fig. 2 *B*), that is, the current at −90 mV was divided by −10.33 pA, and the current at 90 mV was divided by 12.96 pA. To obtain the integral seen in Eq. 5, we naturally measured the area below each of the currents treated as in Fig. 6 *A*. In fact, by doing so, we obtain $N \times \int_0^t P_o(t)\mathrm{d}t$ for each HP.

Fig. 6 *B* shows such integrals for 100-ms pulses of glutamate. To cancel N, all integrals were divided by the one obtained at −90 mV. As seen, for the entire wide range of −90 mV to 90 mV, the integral of P_o increases with depolarization.

Dependence of the dose-response curve on HP

The experiments described so far (excluding the one seen in Fig. 3 *C*) were confined to one glutamate concentration of 10 mM. Fig. 7 *A* shows raw data at a low concentration of 0.5 mM glutamate applied to the same patch shown in Fig. 1 *A*. It can be seen that the effect of HP is much more profound at lower glutamate concentrations (cf. Figs. 7 *A* and 1 *A*).

Fig. 7 *B* shows DR curves obtained at two HPs. The HP for the lower curve (taken from Tour et al., 1995) is at −70 mV. In this curve, each data point represents peak current at a given glutamate concentration normalized to the peak current at 10 mM glutamate; i.e., relative $P_{o(\mathrm{peak})}$. We now explain how the four data points at 90 mV (*upper curve*) were obtained. For each of the four concentrations the peak current was measured, from the same patch, at −70 mV and

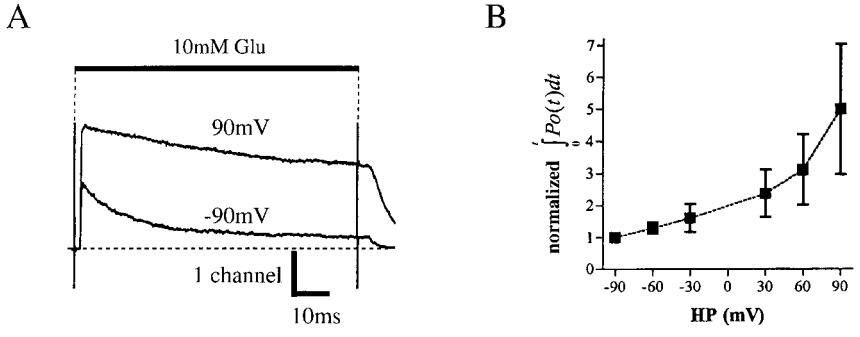

FIGURE 6 Quantitative dependence of P_o on HP. (*A*) To isolate the quantitative dependence of P_o on HP, the other voltage dependent factors (Eq. 5) must be canceled. The pair of currents at HPs of −90 mV and 90 mV from Fig. 1 *A* are used as an example for the procedure of cancellation. The current at −90 mV was divided by the single-channel current recorded at this HP (−10.33 pA; from Fig. 2 *B*), and the same is trues for the current at 90 mV (divided by 12.96 pA; from Fig. 2 *B*). (*B*) Quantitative dependence of P_o on HP expressed as the area under the currents (normalized to the area of the current at −90 mV) for a 100-ms pulse of glutamate. The data are averages of six patches.

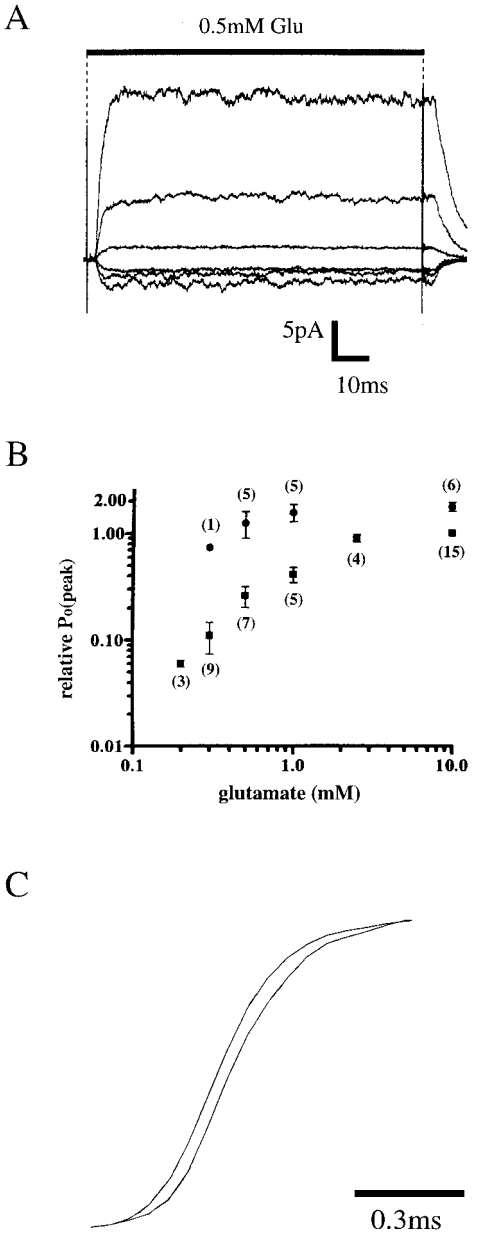

FIGURE 7 Experimental results of the DR and current rising phase. (*A*) Ensemble currents activated by a 100-ms pulse of 0.5 mM glutamate at six different HPs (−90 mV, −60 mV, −30 mV, 30 mV, 60 mV, and 90 mV) obtained from the same patch as seen in Fig. 1 *A*. One hundred two episodes were averaged for each ensemble current. (*B*) Two dose-response curves (DR), one at an HP of −70 mV (●; from Tour et al., 1995) and the other at an HP of 90 mV (■). Each point represents a response normalized to that obtained at 10 mM glutamate, at −70 mV. Furthermore, the points at 90 mV represent the relative rise in $P_{o(peak)}$ at 90 mV, in comparison to its value at −70 mV for each concentration of glutamate. The values (mean ± SD) of the 90-mV DR are 1.75 ± 0.16 for 10 mM, 1.55 ± 0.28 for 1 mM, 1.24 ± 0.35 for 0.5 mM, and 0.74 for 0.3 mM glutamate. The numbers in parentheses, above the data points of the two DR curves, indicate the number of experiments. The two DR curves were fitted by a Hill function (Stryer, 1988) to obtain the glutamate concentration for a half-maximum response. (*C*) Rising phases of two currents at HPs of 90 mV (*left*) and −90 mV (*right*). The currents were each normalized to their peaks (for convenience, the negative current is shown as positive).

90 mV. As we are interested in the effect of HP on $P_{o(peak)}$, the dependence of γ on HP was first accounted for as done in Fig. 6 *A*. Then the ratio of corrected $I_{(peak)}$ at 90 mV to $I_{(peak)}$ at −70 mV for each of the four concentrations was established. Because each of the patches included a different number of channels, the obtained ratios were each multiplied by the lower curve data point at the same concentration. This is because the data points at the lower curve (Tour et al., 1995) were already corrected to account for this aspect. For example, in 10 mM glutamate, the ratio of corrected $I_{(peak)}$ at 90 mV to $I_{(peak)}$ at −70 mV was 1.75 ± 0.16 (six patches analyzed as in Fig. 6 *A*). We therefore multiplied $P_{o(peak)}$ of the lower curve (at 10 mM) by 1.75 to achieve the corresponding point on the DR curve of 90 mV.

Comparing the complete DRs, it can be seen that HP affected, first, the half-maximum response (1.1 mM for HP of −70 mV and 0.34 mM for HP of 90 mV) and, second, the saturation level (1 for HP of −70 mV and 1.75 for HP of 90 mV).

Effect of HP on the rise time of the current

We found that the rise time of the current also depends on HP. As an example, Fig. 7 *C* depicts the rising phases of two currents at the HPs of 90 mV and −90 mV. The currents were normalized to their peaks (for convenience, the negative current was drawn as a positive one). The rise time (5–85%) was found to be 20 μs shorter at 90 mV than at −90 mV. Similar results were obtained in four additional patches where the mean difference in the rise time was 25 ± 16 μs (399 ± 125 μs for −90 mV and 374 ± 120 μs for 90 mV).

Dependence of single-channel kinetics on HP

To unravel the mechanism underlying the dependence of P_o on HP, we evaluated the kinetic properties of single-channel activity at two HPs. Experiments were carried out using the cell-attached configuration under conditions most suitable to detecting fast events (see Materials and Methods). To ensure identification of primary bursts the measurements were made at very low glutamate concentration (0.1 mM). Under such conditions, primary bursts were separated by tens of milliseconds (as exemplified by the gaps seen between consecutive bursts in Fig. 8).

For each patch, data were first collected by employing a command potential of 0 mV (given that the muscle resting potential is around −75 mV, the corresponding patch potential was around −75 mV). When a sufficient amount of data had been collected, a command potential of −180 mV (patch potential ~105 mV) was applied. Fig. 8 shows an example of sequential bursts from one patch at the two command potentials. It is quite apparent that also in cell-attached configuration P_o is higher at the depolarizing patch potential. The higher P_o is reflected in the longer burst duration and in the higher frequency of bursts, evident from

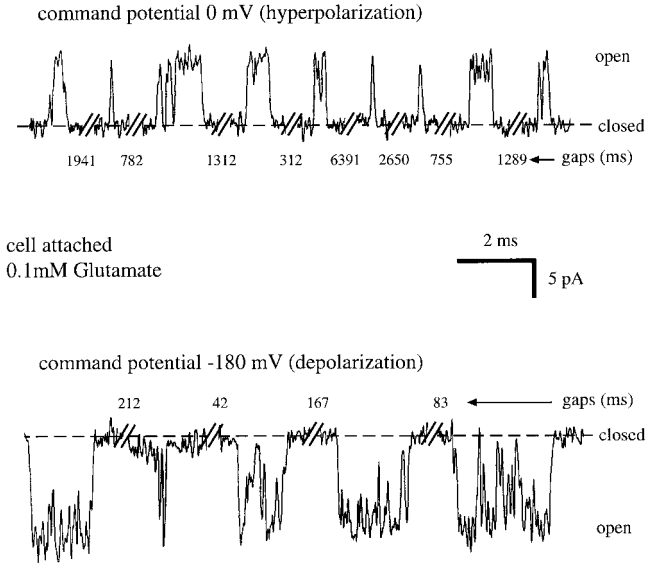

FIGURE 8 Examples of consecutive channel openings in one cell-attached patch in response to 0.1 mM glutamate added to the pipette solution, at two HPs. In the upper trace the command potential was 0 mV, leaving the patch potential equal to the muscle resting potential of ~ −75 mV. Nine consecutive bursts are plotted, with the time elapsed between bursts indicated under the gaps (slashes). In the lower trace the command potential was −180 mV, giving a patch potential of ~105 mV. Five consecutive bursts are plotted, with the time elapsed between bursts indicated above the gaps. Signals were filtered at 10 kHz and digitized at 100 kHz. The noise level during recording was 0.38 pA RMS.

the shorter gaps, at depolarizing patch potential. The mean open time is also longer in this potential (see Table 1). A summary of 10 experiments is provided in Table 1.

Following convention, we can evaluate from the results presented in Table 1 the values of the following rate constants. From the mean open time, the rate constant of channel closing, k_c, can be derived. The rate constant of channel opening, k_o, can be extracted from the mean close time within the bursts. Having established k_o and k_c, we can derive the rate constant of dissociation of glutamate, k_-, from the equation of mean burst duration (Colquhoun and Hawkes, 1981). To do so one needs to know the number of glutamate-binding sites of this receptor. The Hill coefficient of the DR under hyperpolarization was found to be 2.6 (Tour et al., 1995); we therefore considered two cases for the derivation of k_-: one of two binding sites and another of three binding sites. In each of these cases we assumed, in the absence of evidence showing otherwise, that the various dissociation constants are equal. The values of the various rate constants, obtained as described above, are provided in Table 1.

Comparing the evaluated rate constants for depolarization and hyperpolarization, we find that k_- was affected most significantly by membrane potential. It was reduced by 6.5-fold under depolarization. k_c was also significantly affected—it declined by 1.8-fold. k_o was the least affected—it declined by only 1.2-fold.

Does HP also affect the unliganded receptor channel?

To determine whether HP affects the unliganded receptor channel, we conducted experiments like those seen in Fig. 9 *A*. The exact experimental protocol used here was as follows. Starting from a resting potential of −70 mV, a prepulse to a positive value of 70 mV was applied for 16 ms. Glutamate was applied 3.6 ms after the prepulse ended. The evoked current was compared to currents activated by the same glutamate pulse but with various delays after the depolarizing prepulse (7.2 ms, 10.8 ms, 14.4 ms, 18 ms). Fig. 9 *B* depicts superposition of all five currents. The almost complete overlap of the currents indicates that the HP has no effect on the unliganded receptor. To exclude the possibility that a voltage effect does exist but vanishes even during the short delay of 3.6 ms, we repeated the experiment with shorter delays, as can be seen in Fig. 9 *C*. Here the switch to positive HP was made simultaneously with the application of glutamate, slightly before glutamate reached the patch (~100 μs). In Fig. 9 *D* the current seen in Fig. 9 *C* is compared to three additional currents with delays of ~700 μs, ~1300 μs, and ~1900 μs. As for the longer delays (Fig. 9 *B*), all four currents overlap. Similar results were obtained in four additional experiments. Therefore it seems that HP affects only the receptor states that are bound to glutamate.

Time course of the effects of HP

Up to now, the HP was held constant throughout the glutamate pulse. In the following experiments, the HP was altered during the glutamate application to evaluate the time course of its effects. Fig. 10 *A* depicts application of 10 mM

TABLE 1 Effect of HP on single-channel kinetics

	Hyperpolarization	Depolarization
Command potential (mV)	0	−180
Membrane potential (mV)*	−75	105
No. of patches[#]	10	5
Total no. of openings	2034	10940
Mean open time (ms)	0.25 ± 0.03	0.45 ± 0.08
Mean close time in burst (ms)[§]	0.1 ± 0.02	0.12 ± 0.01
Mean burst duration (ms)	0.39 ± 0.06	1.66 ± 0.2
Mean no. of openings in burst	1.4	3.12
k_o (ms^{-1})	10.2	8
k_c (ms^{-1})	4	2.2
k_- ($ms^{-1} \times mM^{-1}$); $H_n = 2$	12.4	1.9
k_- ($ms^{-1} \times mM^{-1}$); $H_n = 3$	8.3	1.26
Mean P_o[¶]	0.00021 ± 0.0001	0.0026 ± 0.0016

*Reversal potential ≈ +15, making the driving force at both potentials ~90 mV.

[#]In depolarization five patches could not been analyzed, because of the high activity of voltage-dependent K^+ channel.

[§]The value of the burst delimiter was taken to be 0.5 ms. This value ensured independence of the number of observed bursts on the value of the burst delimiter.

[¶]P_o was calculated by dividing the sum of the channel openings by the total recording time.

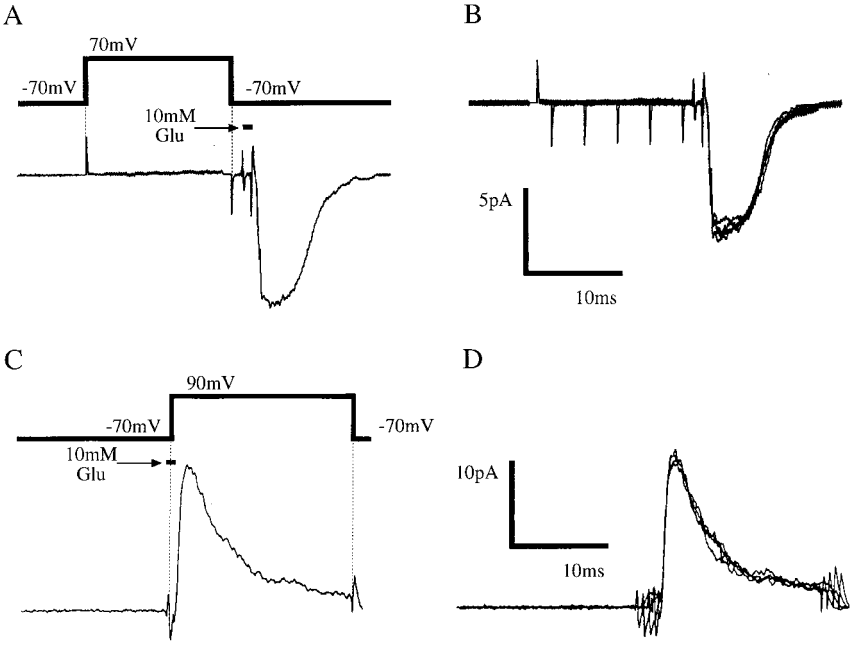

FIGURE 9 The unliganded receptor channel is not affected by HP. (*A*) The voltage protocol is depicted by the heavy upper line. A 1-ms pulse of 10 mM glutamate was applied 3.6 ms after the end of a prepulse of 70 mV, 16 ms. In this figure the vertical dotted line indicates the voltage prepulse. (*B*) The current of *A* is compared to four currents activated by a similar test pulse, but with various delays from the end of the 70-mV prepulse (7.2 ms, 10.8 ms, 14.4 ms, 18 ms). Each current is the outcome of averaging 12 traces. (*C*) Here the switch from −70 mV to a positive HP of 90 mV was done simultaneously with the application of glutamate, slightly before glutamate reached the patch (~100 μs). (*D*) The current of *C* is compared to three additional currents with delays of ~700 μs, ~1300 μs, and ~1900 μs. Signals were digitized at 50 kHz.

glutamate for 60 ms; after 40 ms the HP was switched from 90 mV to −70 mV. For comparison, in Fig. 10 *B*, the HP was kept at −70 mV throughout the glutamate application (control). The two currents are superimposed in Fig. 10 *C*. The current immediately after the voltage switch was twice that of the control. Notice that at this time, HP and γ are identical for both currents; hence the higher current reflects solely a higher P_o. The full rise in the current cannot be measured, because of amplifier saturation, which lasts for 1 ms (see *voltage switch* in Fig. 10, *A* and *C*). It can be calculated, however, as P_o changes slowly in comparison with the immediate change in γ on switching HP. The current immediately after the switch is given by the product of the current amplitude just before the switch multiplied by the ratio of the single-channel currents at the two HPs (−10.33 pA/12.96 pA, from Fig. 2 *B*). The value thus obtained is marked by an asterisk in Fig. 10, *A* and *C*. Similar results were obtained in four other experiments.

The finding that the current after switching from 90 mV to −70 mV was higher than control (Fig. 7 *C*) indicates that the involved rate constants have slow time constants in comparison to the rapid voltage change. Or, in other words, the system possesses a "memory." To demonstrate a case in which the current after the voltage switch is actually higher than with constant hyperpolarization, we selected a case in which the memory is more profound; i.e., a lower glutamate concentration (see Fig. 7 *B*). Fig. 10 *D* shows such a case. Here a glutamate concentration of 0.75 mM was applied for 10 ms. In one case after 7 ms of glutamate application, the HP was switched from 30 mV to −70 mV. In the second case the HP was maintained at −70 mV throughout glutamate application. Potentiation of P_o by depolarization to 30 mV increased the peak current after the voltage switch by 70%.

The effect of a rapid change in HP from hyperpolarization to depolarization was also examined. This shows the time course of resensitization from the more desensitized mode at hyperpolarization to a less desensitized mode at depolarization (Fig. 10, *E–G*). In Fig. 10 *E* the HP was switched from −70 mV to 90 mV 10 ms after the beginning of glutamate application. During these 10 ms, the current desensitized down to 13% of its peak level. After the switch, the current recovered to a steady-state level corresponding to 90 mV (30% of the peak). A time constant of 5 ms was fitted to the recovery process.

Fig. 10 *F* gives the control for the experiment in Fig. 10 *E*, where an HP of 90 mV was maintained throughout the glutamate application. Fig. 10 *G* illustrates superposition of the currents obtained under the two experimental protocols. Also seen in Fig. 10 *G* are currents corresponding to three additional rapid voltage changes (25 ms, 40 ms, and 55 ms after the beginning of glutamate application). In all cases, the current recovered to the steady-state level corresponding to 90 mV.

DISCUSSION

We present here a comprehensive study in which the dependencies of γ and P_o on membrane potential were evaluated. In this study γ was directly measured at a wide range of HPs. These measurements enabled us, for the first time, to show directly the increase in γ at positive HPs. We ascertained the dependence of γ on HP also in cell-attached patches. By establishing γ, we could isolate the effect of membrane potential on P_o itself from ensemble currents. The complex dependence of P_o on HP was also studied at the single-channel level to reveal the various rate constants affected by the HP.

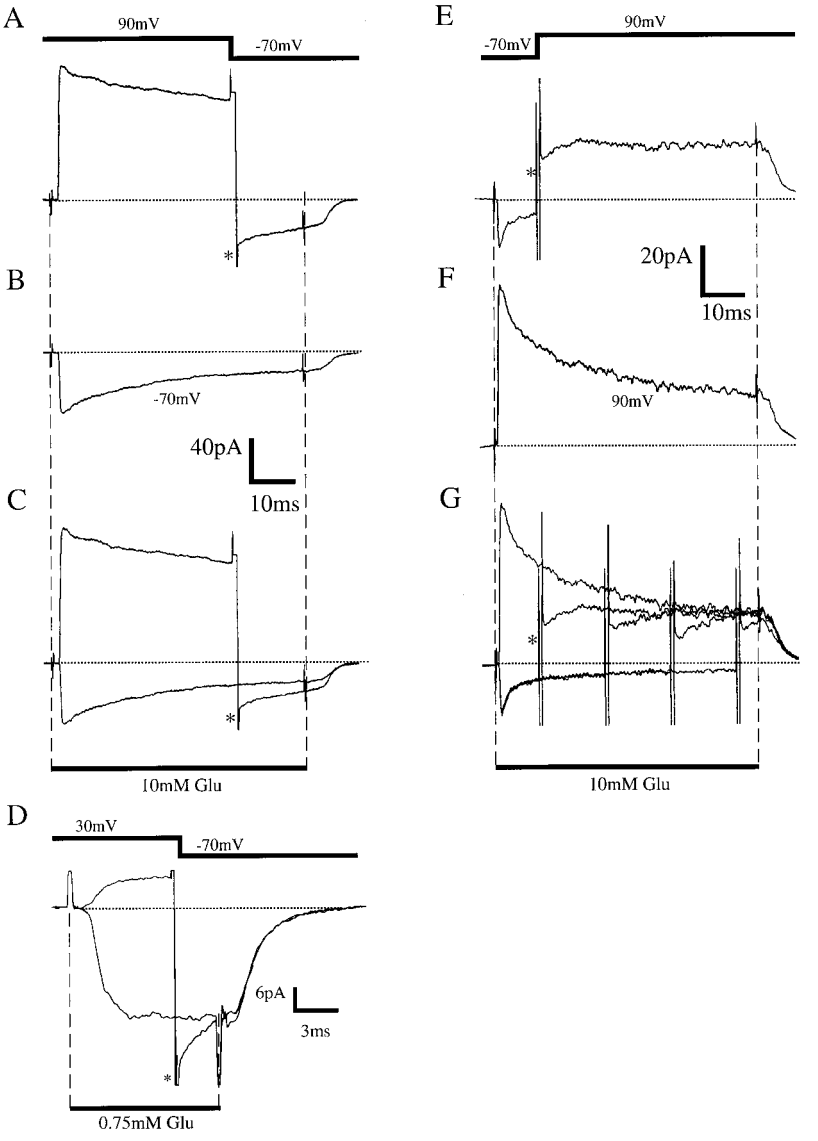

FIGURE 10 Effects of changing the HP during glutamate application. (*A*) Application of 10 mM glutamate for 60 ms; after 40 ms the HP was switched from 90 mV to −70 mV (the voltage protocol is given above the current traces). (*B*) Glutamate application for 60 ms at constant HP of −70 mV is shown for comparison. (*C*) Superposition of *A* and *B*. (*D*) A superposition of two currents activated by the application of 0.75 mM glutamate for 10 ms. In one current, after 7 ms of glutamate application, the HP was switched from 30 mV to −70 mV. In the second current the HP was maintained at −70 mV throughout glutamate application. Potentiation of P_o by depolarization to 30 mV increased the peak current after the voltage switch by 70%. Ninety episodes were averaged for each ensemble current, filtered at 2 kHz, and digitized at 33 kHz. (*E*) The effect of switching from hyperpolarization to depolarization. HP was switched from −70 mV to 90 mV, 10 ms, after the beginning of glutamate application (voltage protocol is above the current). (*F*) The same glutamate application as in *E*, but with a constant HP of 90 mV, is shown for comparison. (*G*) Superposition of *E* and *F*, together with currents corresponding to three additional voltage switches (25 ms, 40 ms, and 55 ms after the beginning of glutamate application). Sixty episodes were averaged for each ensemble current in *A*, *B*, *C*, *E*, *F*, and *G*.

In earlier studies on quisqualate channels in crayfish, γ was reported to be independent of voltage (Franke et al., 1987). A single slope of 100 pS was fitted to the data, which is similar to the slope reported here for negative HPs. As Franke et al. (1987) focused mainly on the hyperpolarization range of membrane potentials, it is possible that they could not have detected the nonlinearity of the *I-V* curve observed here.

Conflicting results have been obtained for other non-NMDA channels. For example, in various neuron types from rat hippocampus, Colquhoun et al. (1992) found a linear peak current-to-voltage relation, implying that γ is independent of HP. In contrast, in chick embryos, Raman et al. (1995) found that γ increased by ~50% at a depolarization of +60 mV in comparison to its value at −60 mV. This elevation in γ is lower than the 90% increase observed in our studies. The difference may reflect intrinsic variations in the properties of the glutamate receptors in the two preparations. Alternatively, the difference may be due to the use of different experimental methods. Raman et al. (1995) used a nonstationary variance analysis, which is an indirect method for evaluating single-channel currents, whereas we evaluated γ directly from single-channel recordings (see Fig. 2).

Similar to our findings, earlier studies indicated that P_o increases with depolarization; it was shown in the crayfish that the decay phase of the Excitatory Post Synaptic Current is prolonged under depolarization (Dudel, 1974; Onodera and Takeuchi, 1978; Dudel, 1979). The dependence of P_o on depolarization was later confirmed by using the cell-attached configuration (Dudel and Franke, 1987). Raman and Trussell (1995) showed a voltage sensitivity of glutamate neurons of the avian cochlear nucleus. They favored the explanation that P_o increases because of slowing of channel gating, suggesting that the channels may exist in different open states and that depolarization increases the proportion of time that the channels spend in a longer lasting open state.

Using single-channel measurements, we could resolve the effect of depolarization on the three rate constants that can be estimated from single-channel recordings: k_-, k_c, and k_o. This does not mean that membrane potential does not affect other rate constants. It is therefore interesting to see whether the effect of depolarization on the DR and on the rise time can also be explained by the changes in these three rate constants.

We find that, indeed, the changes seen in the three rate constants can account qualitatively for the increase in the saturation level and the shift to the left of the DR. The stronger decline in k_c in comparison to that of k_o guarantees that the saturation level increases, as this level is determined by $k_o/(k_o + k_c)$. The shift of the DR to the left and the rather small shortening of the rise time can be accounted for by the large reduction in k_- (Franke et al., 1991).

Despite the qualitative agreement there is a quantitative discrepancy concerning the level of saturation of the DR. The reduction seen in k_c (1.8-fold) and in k_o (1.2-fold) predicts an increase of 18% in the level of saturation. The experimental rise in the level of saturation was much higher (75%) than this predicted one. This discrepancy can be accounted for partly by the built-in experimental imprecision in evaluating k_o. With the extremely brief bursts under hyperpolarization and the closing within the burst being on the limit of possible resolution, the evaluation of k_o is not very safe. Another possible source for a larger than predicted difference in the level of saturation could be the faster desensitization under hyperpolarization. Assuming, like others before (Franke et al., 1993), that desensitization occurs from the open state, and including the time constants of desensitization measured here, we found that the peak current would decline by ~3% because of desensitization. Desensitization, therefore, cannot be considered as a major effect on the level of saturation. Furthermore, the two effects together leave the observed quantitative discrepancy unresolved.

As shown, depolarization also affects desensitization. Our results (Fig. 4) suggest that it is not the time constant of desensitization that is affected. One possible explanation to these results is that two states of receptors (or two processes) exist, each with its own fixed time constant of decay, and the HP determines the balance between the two states (processes). At extreme negative HPs, the state with a small time constant of decay dominates, whereas, at extreme positive HPs, the state with a larger time constant dominates. Raman and Trussell (1995) obtained similar results and reached the same conclusions concerning AMPA channels.

Our findings have a possible physiological significance. In the various experiments we demonstrated significant differences in channel behavior under different HPs. Fig. 10 also shows that if a voltage switch occurs during glutamate application, the channels maintain, for a few milliseconds afterward, the properties corresponding to the HP that preceded the switch. Because of this "memory," postsynaptic facilitation may occur, provided that a "physiological voltage switch" takes place.

One example of a possible physiological voltage switch is the following. Excitatory postsynaptic potentials (EPSPs) of up to 80 mV (from −70 mV to +10 mV) were recorded from the deep abdominal extensor muscle of the crayfish (Parnas and Atwood, 1966). This muscle is innervated by more than one excitatory axon. If the postsynaptic muscle is depolarized because of the activity of any number of presynaptic neurons, and simultaneously, at the peak of the depolarization (synaptic potential, +10 mV) a particular presynaptic neuron releases glutamate, the postsynaptic channels will exhibit a memory and show potentiation that will take place after repolarization.

However, in this example, the velocity of the physiological voltage switch is too slow (~10 ms), and most of the potentiation in P_o will vanish before the membrane is repolarized.

A much more profound postsynaptic facilitation is expected in neuron-neuron synapses. There, the physiological voltage switch is the action potential, which exhibits a fast time course in comparison to the neuromuscular EPSP. The question is, does a "memory" such as the one reported here actually exist in neuron-neuron synapses? Suggestive evidence in this direction has been reported, but not interpreted in this context, by Jonas and Sakmann (1992; see Fig. 5).

In conclusion, taking into account the well-established fact that non-NMDA channels comprise a major fraction of the postsynaptic excitatory channels (Kandel and Schwartz, 1991), the data presented here suggest that hebbian learning can also be achieved by non-NMDA channels.

This research was supported by the Deutscheforschungsgemeinschaft, Germany (grant SFB 391).

REFERENCES

Bowie, D., and M. L. Mayer. 1995. Inward rectification of both AMPA and kainate subtype glutamate receptors generated by polyamine-mediated ion channel block. *Neuron.* 15:453–462.

Colquhoun, D., and A. G. Hawkes. 1981. On the stochastic properties of single ion channels. *Proc. R. Soc. Lond. B.* 211:205–235.

Colquhoun, D., P. Jonas, and B. Sakmann. 1992. Action of brief pulses of glutamate on AMPA/kainate receptors in patches from different neurones of rat hippocampal slices. *J. Physiol. (Lond.).* 458:261–287.

Dudel, J. 1974. Nonlinear voltage dependence of excitatory synaptic current in crayfish muscle. *Pflügers Arch.* 352:227–241.

Dudel, J. 1979. The voltage dependence of the decay of the excitatory post-synaptic current and the effect of concanavalin A at the crayfish neuromuscular junction. *J. Physiol. (Paris).* 75:601–604.

Dudel, J., and C. Franke. 1987. Single glutamate-gated synaptic channels at the crayfish neuromuscular junction. II. Dependence of channel open time on glutamate concentration. *Pflügers Arch.* 408:307–314.

Dudel, J., C. Franke, and H. Hatt. 1990. Rapid activation, desensitization, and resensitization of synaptic channels of crayfish muscle after glutamate pulses. *Biophys. J.* 57:533–545.

Franke, C., and J. Dudel. 1987. Single glutamate-gated synaptic channels at the crayfish neuromuscular junction. I. The effect of enzyme treatment. *Pflügers Arch.* 408:300–306.

Franke, C., H. Hatt, and J. Dudel. 1987. Liquid filament switch for ultra-fast exchanges of solutions at excised patches of synaptic membrane of crayfish muscle. *Neurosci. Lett.* 77:199–204.

Franke, C., H. Hatt, H. Parnas, and J. Dudel. 1991. Kinetic constants of the acetylcholine (ACh) receptor reaction deduced from the rise in open probability after steps in ACh concentration. *Biophys. J.* 60:1008–1016.

Franke, C., H. Parnas, G. Hovav, and J. Dudel. 1993. A molecular scheme for the reaction between acetylcholine and nicotinic channels. *Biophys. J.* 64:339–356.

Hamill, O. P., A. Marty, E. Neher, B. Sakmann, and F. J. Sigworth. 1981. Improved patch-clamp techniques for high-resolution current recording from cells and cell-free membrane patches. *Pflügers Arch.* 391:85–100.

Hestrin, S., R. A. Nicoll, D. J. Perkel, and P. Sah. 1990. Analysis of excitatory synaptic action in pyramidal cells using whole-cell recording from rat hippocampal slices. *J. Physiol. (Lond.).* 422:203–225.

Jonas, P., and B. Sakmann. 1992. Glutamate receptor channels in isolated patches from CA1 and CA3 pyramidal cells of rat hippocampal slices. *J. Physiol. (Lond.).* 455:143–171.

Kandel, E. R., and J. H. Schwartz. 1991. Directly gated transmission at central synapses. *In* Principles of Neural Science, 3rd Ed. E. R. Kandel, J. H. Schwartz, and T. M. Jessell, editors. Elsevier Science Publishing Co., New York. 153–172.

Keller, B. U., A. Konnerth, and Y. Yaari. 1991. Patch clamp analysis of excitatory synaptic currents in granule cells of rat hippocampus. *J. Physiol. (Lond.).* 435:275–293.

Livsey, C. T., E. Costa, and S. Vicini. 1993. Glutamate-activated currents in outside-out patches from spiny versus aspiny hilar neurons of rat hippocampal slices. *J. Neurosci.* 13:5324–5333.

Magleby, K. L., and C. F. Stevens. 1972. The effect of voltage on the time course of end-plate currents. *J. Physiol. (Lond.).* 223:151–171.

Mayer, M. L., and G. L. Westbrook. 1984. Mixed-agonist action of excitatory amino acids on mouse spinal cord neurones under voltage clamp. *J. Physiol. (Lond.).* 354:29–53.

Nowak, L., P. Bregestovski, and P. Ascher. 1984. Magnesium gates glutamate-activated channels in mouse central neurones. *Nature.* 307: 463–465.

Onodera, K., and A. Takeuchi. 1978. Effects of membrane potential and temperature on the excitatory post-synaptic current in the crayfish muscle. *J. Physiol. (Lond.).* 276:183–192.

Parnas, I., and H. L. Atwood. 1966. Phasic and tonic neuromuscular systems in the abdominal extensor muscles of the crayfish and rock lobster. *Comp. Biochem. Physiol.* 18:701–723.

Patneau, D. K., L. Vyklicky, and M. L. Mayer. 1993. Hippocampal neurons exhibit cyclothiazide-sensitive rapidly desensitizing responses to kainate. *J. Neurosci.* 13:3496–3509.

Raman, I. M., and L. O. Trussell. 1995. Concentration-jump analysis of voltage-dependent conductances activated by glutamate and kainate in neurons of the avian cochlear nucleus. *Biophys. J.* 69:1868–1879.

Stryer, L. 1988. Biochemistry, 3rd Ed. W. H. Freeman and Company, New York. 154–156.

Tour, O., H. Parnas, and I. Parnas. 1995. The double ticker: an improved fast drug-application system reveals desensitization of the glutamate channel from a closed state. *Eur. J. Neurosci.* 7:2093–2100.

Watkins, J. C. 1994. The NMDA receptor concept: origins and development. *In* The NMDA Receptor, 2nd ed. G. L. Collingridge and J. C. Watkins, editors. Oxford University Press, New York. 1–30.